Protocol Modeling for On-body Delay Tolerant Routing in Wearable Sensor Networks

[1]*Muhannad Quwaider*, [2]*Mahmoud Taghizadeh, and* [2]*Subir Biswas*
[1]*Computer Engineering, Jordan University of Science and Technology, Irbid, Jordan*
[2]*Electrical and Computer Engineering, Michigan State University, East Lansing, Michigan, USA*

Abstract - This paper presents a stochastic modeling framework for store-and-forward packet routing protocols in Wireless Body Area Networks (*WBAN*). A prototype *WBAN* has been constructed for experimentally characterizing and capturing on-body topology disconnections in the presence of ultra short range radio links, unpredictable RF attenuation, and human postural mobility. Delay modeling techniques for evaluating single-copy on-body DTN routing protocols are then developed. End-to-end routing delay for a series of protocols including opportunistic, randomized, utility-based and other mechanism that capture multi-scale topological localities in human postural movements has been evaluated. Performance of the analyzed protocols is then evaluated experimentally to compare with the results obtained from the developed model.

Keywords: Wearable Sensor Network, Delay Tolerant Network

I. INTRODUCTION

Short transmission range is a common constraint for low-power RF transceivers designed for embedded applications with limited energy [1], often supplied by harvested operations [2]. Such situations are particularly pertinent for implantable body sensors. Examples of ultra-low range transceivers in the literature include [1] with 0-1m, [2] with 0.2-1m, [3] with 0.2m, and [4] with 0-1m transmission ranges. The corresponding transmission powers vary between 0.75mW to 6mW, which are within a range that can be handled with common harvesting techniques such as piezo-electric generation from body movements.

Low RF ranges also mean that body movements can give rise to frequent partitioning or disconnection in Wireless Body Area Network (WBAN) topologies, resulting in a body area Delay Tolerant Network (DTN) [5]. Such topological partitioning can often get aggravated by the unpredictable RF attenuation caused due to signal blockage by clothing material and body segments. The goal of this paper is to develop analytical modeling mechanisms for computing packet transfer delay for a series of DTN routing algorithms that can be implemented in an on-body setting.

The existing research on routing in Delay Tolerant Networks or DTNs are categorized [5]as: 1) replication based (multiple copy) [6], and 2) single copy [7], [8]. The replication approach explores the ways in which several copies of a packet can be disseminated among several carrier mobile nodes to increase the chance of delivery to the desired destinations. Most of routing schemes proposed for DTN routing protocols belong to this category [6], [9]. While providing good delay performance, the primary limitation of these protocols is their energy and capacity overheads due to excessive packet transmissions. For ultra resource-constrained WBANs, such overheads are usually not acceptable. The single copy forwarding mechanisms make use of information about the connectivity and topology dynamics to make low-latency forwarding decisions with minimal replication overhead. The general principle is that when a node with a buffered packet encounters another node, the packet is forwarded to the encountered node only if it is more likely (than the node currently buffering the packet) to visit the destination node.

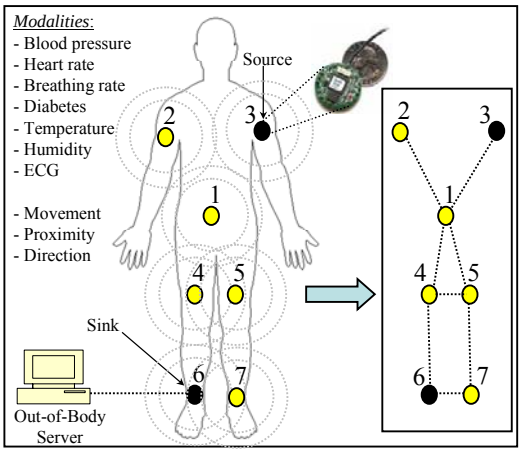

Fig. 1: Body Area Sensor Network

For the above mechanisms to work as anything beyond epidemic/viral routing [10], the nodes need to have certain degree of spatial and temporal locality in their mobility and meeting patterns. A notable DTN routing scheme in the literature is PROPHET [6] which is an extension of epidemic routing [9]. PROPHET develops a probabilistic framework for capturing the spatio-temporal locality present in the node mobility pattern within a dynamically partitioned wireless network. PROPHET can be implemented either in single copy or in multi-cope mode. Node interaction localities can be also captured in the form a per-link *utility* as detailed in [11], [7]. The link utility can be formulated as its age [7], [8], [12], formation frequency [7], and other historical parameters that can effectively capture the nodes' interaction localities.

Two additional routing protocols, namely *opportunistic* [11], [12], [7] and *randomized* [12], [7] are also analyzed in the literature for applications in which either there is no node-interaction locality or such localities can not be evaluated. With opportunistic routing, a source node directly delivers its packets to the destination node, and buffers them till the link with the destination is formed. In randomized routing, packets are randomly routed following the hot-potato logic [12]. Both these protocols are hugely outperformed by the locality based protocols [12], [7] due to their knowledge about the properties of the links.

In this paper, however, a key goal is to formulate modeling mechanisms that can capture multi-scale topological localities in human postural movements, and use such locality information for modeling packet routing delay. In addition to general purpose DTN routing, including opportunistic [11], [12], [7], utility based [8], [12], [7],, random [12], [7] one other protocol, PRMPL [13], which is specifically designed for on-body DTN routing is also modeled in this paper.

II. EXPERIMENTAL CHARACTERIZATION

A. WBAN Prototype

A *Wireless* Body Area Network (*WBAN*) is constructed by

mounting seven sensor nodes (attached on two upper-arms, two thighs, two ankles and one in the waist area) as shown in Fig. 1. Each wearable node consists of a 900MHz Mica2Dot MOTE (running TinyOS operating system), with Chipcon's SmartRF CC1000 radio chip (chipcon.com), and the sensor card MTS510 from Crossbow Inc. (www.xbow.com). The Mica2Dot nodes run from a 570mAH button cell with a total sensor weight of approximately 10 grams. The default CSMA MAC protocol is used with a data rate of 19.2kbps.

Via software adjustments of the CC1000's transmission power, the transmission range is set to be in between 0.3m-0.6m. By doing so, we are able to emulate the ultra-low transmission range for the embedded transceivers [2], [1], [3], [4] as reported in the literature. Note that the variation of the range is caused due to the variability in antenna orientation, clothing, and other on-body RF attenuation characteristics.

All experiments in this paper correspond to multi-point-to-point routing in which data from all other nodes are sent to node-6 (see Fig. 1), which is designated as the on-body sink node. This node collects raw data, and sends processed results to an out-of-body server using a wireless link. This external link is created between the on-body sink and to an out-of-body Mica2Dot node connected to a PC through a custom-built serial interface, running RS232 protocol.

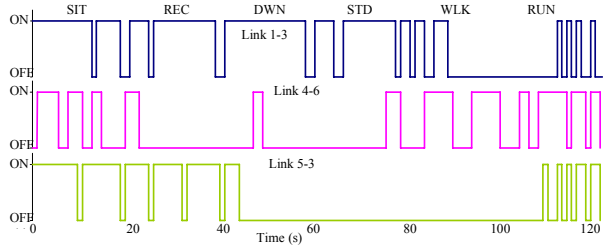

Fig. 2: Variation of instantaneous link connectivity with postural mobility

B. *Variations of Topology and Network Partitions*

A subject, fitted with seven sensors, was asked to follow a pre-determined posture sequence (SIT, SIT-RECLINING, LYING-DOWN, STAND, WALK and RUN), each lasting for 20 sec. The status of three WBAN links (1-3, 4-6, and 5-3) during such an experiment is shown in Fig. 2.

The following observations can be made from Fig. 2. First, few links are connected only during certain postures, which can lead to significant topology variations and network partitioning across the postures. For instance, link 5-3 (between left front thigh and upper left arm nodes) shows the effect of distance on connectivity. The link is connected during most closed postures such as SIT and REC. However, for the stretched out postures such as LYING-DOWN, STAND and WALK, the link is mostly disconnected. Similar trends are observed for the other links including link 1-3 and link 4-6, as shown in Fig. 2.

The second observation is that even within a posture, a link may have intermittent disconnections (e.g. link 1-3 is disconnected during the SIT posture from '0-20' sec. interval). The reasons for such intra-posture disconnections include minor body movements, RF signal blockage by body segments and clothing material, and also the relative orientations of the node-pairs forming the link in question.

C. *Topology Trace Collection*

An objective of this paper is to develop delay models for different DTN routing protocols executed on dynamic *WBAN* topologies as depicted in Fig. 2. A remote trace collection mechanism was developed so that real network topology traces from the prototype *WBAN* can be wirelessly collected and used for routing model development.

During the on-body experiments, the state of each link (emulated using limited transmission power as shown in Fig. 2) is periodically sent to the out-of-body server at full transmission power. The server collects the link-state samples (ON or OFF) from all the on-body links and stores them with a time-stamp from its local clock. All these link-state samples, together, form topology traces which are then used for delay model development as presented in *Section III*. Results from the delay model are compared with the routing performance from the on-body experiments since all of them use the exact same topology traces, ensuring comparable link state and network partitioning patterns as discussed through the example in Fig. 2.

III. MODELING DTN ROUTING PROTOCOLS

Definition 1 (Link State): The state of a link between two nodes *i* and *j* at the n^{th} discrete time slot is represented as $L_{i,j}(n)$, which is assigned the value 1 or 0 to indicate the state to be connected or disconnected respectively.

Definition 2 (Link Disconnection Probability): The Link Disconnection Probability (LDP) for the link between node-*i* and node-*j* is represented as $\hat{P}_{i,j}(k)$. The quantity $\hat{P}_{i,j}(k)$ represents the probability that after an arbitrarily chosen time slot, the link remains disconnected for *k* consecutive disconnected time slots. In a sufficiently long topology trace, spanning *T* time slots, if n_k represents the number of occurrences of such *k*-slot long disconnections, then the LDP can be expressed as:

$$\hat{P}_{i,j}(k) = \begin{cases} n_k / T, & for\ k \geq 1 \\ \sum_{n=1}^{T} L_{i,j}(n) \Big/ T, & for\ k = 0 \end{cases} \quad (1)$$

The case $k \geq 1$ represents situations for which the arbitrarily chosen slot is a part of one of the T_{off} periods (except the last slot on the T_{off} period) or the last slot during one of the T_{on} periods. Similarly, the case $k = 0$ represents situations for which the arbitrarily chosen slot is a part of one of the T_{on} periods (except the last slot on the T_{on} period) or the last slot during one of the T_{off} periods. With above definition of $\hat{P}_{i,j}(k)$, we have $\sum_{k=0}^{T} \hat{P}_{i,j}(k) = 1$, and its expected value can be represented as: $ELD_{i,j} = \sum_{k=0}^{T} k \cdot \hat{P}_{i,j}(k)$, (2)

which is the mean Link Delay, representing the average number of disconnection slots after an arbitrarily chosen slot. $ELD_{i,j}$ can be also expressed as $T_{off}^{i,j}/2$, where $T_{off}^{i,j}$ is the average disconnection duration for link *i* to *j*.

A. *Opportunistic Routing*

In opportunistic routing (OPPT) [11], [12], [7] a source node delivers packet to the destination node only when the two nodes come into direct contact. This single copy mechanism offers a simple DTN routing approach for which the delay can be very large, especially in scenarios with low mobility or infrequent link formation between the source and destination. As done in [7], the opportunistic routing is modeled and analyzed in this section for estimating the worst delay performance when complex algorithms need to be avoided for the resource-constrained on-body sensors.

Since a source node *s* delivers a packet to destination *d* only when $L_{s,d} = 1$ and a packet at node *s* can be generated at any arbitrary time slot, the delivery delay for a packet is $ELD_{s,d}$ as

developed in Eqn. 2. This is true only when the packet generation rate is low enough so that no more than one packet is generated during a T_{off} period. This means that the packet can be delivered at the very beginning of the following T_{on} period without any additional wait.

However, when the packet generation rate is higher so that multiple packets are generated during a T_{off} period, the packets need to be delivered one per time slot during the next T_{on} period. This backlog clearance adds an additional delay component that needs to be added in addition to the $ELD_{s,d}$ from Eqn. 2. Let B represent the number of packets generated during the T_{off} period. With λ being the packet generation rate at the source node s, $B = \lambda \cdot T_{off}$. After the subsequent T_{on} period starts, these B packets are flushed one packet per time slot, requiring B time slots. During these B slots, another $B.\lambda$ packets are generated which are then cleared one per slot.

Combining the backlog clearance delay with the Expected Link Delay (ELD), the average delivery delay for the packets generated during the T_{off} period can be written as $ELD_{sd} + \sum_{i=1}^{B-1} i \Big/ B$. Average delay for the packets generated during the T_{on} period can be written as $\frac{B}{2} + \sum_{i=1}^{B\lambda-1} i$. Therefore, the overall average packet delay for on-body opportunistic routing can be expressed as:

$$D_{OPPT} = \frac{B \cdot \left(ELD_{sd} + \sum_{i=1}^{B-1} i \right) + B \cdot \lambda \cdot \left(\frac{B}{2} + \sum_{i=1}^{B\lambda-1} i \right)}{B + B \cdot \lambda}, \quad (3)$$

where Expected Link Delay (ELD) can be computed in Eqn. 2, and $B = \lambda \cdot T_{off}^{s,d} = 2 \cdot \lambda \cdot ELD_{s,d}$. This expression is valid when the system is stable in the sense that on an average, all packets generated during the T_{on} and T_{off} periods are able to be delivered during the T_{on} period.

B. Randomized Routing

In a randomized routing protocol (RAND), if a node with a data packet does not have a direct connection with the destination, the node forwards the data packet to a neighbor chosen at random [12], [7]. The packet is subsequently forwarded in the same way, till it is received at the destination.

<u>*Definition 3 (Forwarding Probability)*:</u> In RAND forwarding, a node-*i* forwards a packet uniformly randomly to one of its currently connected neighbors. Therefore, at any time slot *n*, the probability of node *i* forwarding a packet to node *j* is defined as:

$$P_{i,j}^{f}(n) = \frac{L_{i,j}(n)}{\sum_{j=1}^{N} L_{i,j}(n)}, \; for\ all\ j \in N,\ j \neq i,\ j \neq d \quad (4)$$

where N is the number of nodes in the network. Eqn. 4 is applicable as long as node i currently has at least one neighbor $\left(i.e. \sum_{j=1}^{N} L_{i,j}(n) \neq 0 \right)$ and none of those neighbors is the destination d $\left(i.e.\, L_{i,d}(n) = 0 \right)$. In case when node i has d as a current neighbor, the packet is forwarded to node d with probability '1'. Also, when node i has no current neighbors, it keeps buffering the packet $\left(i.e. P_{i,i}^{f}(n) = 1 \right)$, resulting in $P_{i,j}^{f}(n) = 0,\ for\ all\ j \neq i$.

<u>*Definition 4 (Forwarding Matrix)*</u>: This matrix captures the forwarding probabilities at time slot *n* across all possible links in the network with *N* nodes and can be represented as shown in Eqn. 5.

$$A(n) = \begin{bmatrix} & 1 & 2 & \cdots & j & \cdots & N \\ 1: & P_{1,1}^{f}(n) & P_{1,2}^{f}(n) & \cdots & P_{1,j}^{f}(n) & \cdots & P_{1,N}^{f}(n) \\ 2: & P_{2,1}^{f}(n) & P_{2,2}^{f}(n) & \cdots & P_{2,j}^{f}(n) & \cdots & P_{2,N}^{f}(n) \\ \vdots & \vdots & \vdots & \cdots & \vdots & \cdots & \vdots \\ i: & P_{i,1}^{f}(n) & P_{i,2}^{f}(n) & \cdots & P_{i,j}^{f}(n) & \cdots & P_{i,N}^{f}(n) \\ \vdots & \vdots & \vdots & \cdots & \vdots & \cdots & \vdots \\ d: & 0 & 0 & \cdots & 0 & \cdots & 0 \\ \vdots & \vdots & \vdots & \cdots & \vdots & \cdots & \vdots \\ N: & P_{N,1}^{f}(n) & P_{N,2}^{f}(n) & \cdots & P_{N,j}^{f}(n) & \cdots & P_{N,N}^{f}(n) \end{bmatrix} \quad (5)$$

The Forwarding Matrix *A(n)* has two notable properties. First, the elements in the d^{th} row are all zeros since the destination node *d* never forwards a packet. The elements in the d^{th} column, however, are either 1 or zero (not explicitly shown above), depending on node *d*'s instantaneous connectivity with the other nodes as expressed above in Eqn. 4. Second, the summation of all elements in all rows (except the d^{th} row) should be 1. The Forwarding Matrix can be created after the forwarding probabilities are computed using Eqn. 4 based on the observed link states from the collected WBAN topology traces.

Consider a packet that is generated at node *s* during the n^{th} time slot, and delivered to node *d* at the $(n+k)^{th}$ time slot, resulting in a delay of *k* slots. The value of *k* can vary from 0 to infinity. Let the probability of delivering the packet with a delay of *k* slots be represented as the delivery probability $\rho_{s,d}^{n}(k)$, which can be written as:

$$\rho_{s,d}^{n}(k) = \left[A(n).A(n+1).....A(n+k) \right]_{s,d} = \left[\prod_{i=0}^{k} A(n+i) \right]_{s,d} \quad (6)$$

which is the [s,d] element of the product matrix. Therefore the expected RAND forwarding delay for a packet that was generated at the n^{th} time slot can be written as:

$$D_{RAND} = \sum_{k=0}^{T} k.\rho_{s,d}^{n}(k) = \sum_{k=0}^{T} k. \left[\prod_{i=0}^{k} A(n+i) \right]_{s,d} \quad (7)$$

where *T* is the length of the experimental topology traces obtained in *Section II.C.* Considering sufficiently long on-body topology traces (i.e. large *T*), the maximum value of *k* in Eqn. 7 is set to be *T* instead of infinity.

C. Utility-based Routing using Link Locality

In randomized routing, a node does not consider the locality of its connectivity with other network nodes while forwarding a packet. In utility based routing protocols [6], [12], [7], [11], [8] nodes prefer to forward packets to destination through the neighbor with the latest encounter with the destination, thus leveraging the link locality in the form of its age. Each node is assigned a utility value based on the last encounter time with the destination, and a packet is forwarded to a neighbor with the highest utility value. Utility represents how useful (fast) this node might be in delivering a data packet to the destination, and is often implemented using a timer.

Let the utility function $U_{i,j}(n)$ represent the utility value of node *i* with respect to node *j* at the n^{th} time slot. Every time node *i* comes in contact with node *j*, the quantity $U_{i,j}(n)$ is set to a maximum utility value and then for every time slot the node remains out of contact from the destination, the quantity $U_{i,j}(n)$ is decreased based on a pre-set utility reduction method [7], [8] as a function of elapsed time. The update rule for $U_{i,j}(n)$ can be written as:

$$U_{i,j}(n+1) = \begin{cases} U_{\max}, & if\ L_{i,j}(n+1) = 1 \\ U_{i,j}(n) - 1, & if\ L_{i,j}(n+1) = 0 \end{cases} \quad (8)$$

where U_{max} is the maximum possible utility value to the destination. These utility values are exchanged between neighbors within the periodic *Hello* messages.

With this definition of utility, at the n^{th} time slot node-*i* will forward a packet (destined to node-*d*) to node-*j* only if $U_{i,d}(n) < U_{j,d}(n)$ and $U_{j,d}(n) \geq U_{k,d}(n), \forall k \in \psi_i(n)$, where $\psi_i(n)$ is all neighbors of node-*i* during the n^{th} slot.

Note that the above forwarding logic assumes that each on-body node is guaranteed to intermittently come within up to 2-hop contact from the destination node. In other words, a source node is able to meet other nodes that intermittently come in direct contact with the destination node. In our experimental topology this assumption was always found true [13]. In fact for a WBAN topology, it is generally true that depending on the specific postural patterns, all nodes intermittently form direct links with all other nodes in the network. This observation makes the assumption generally applicable for WBANs which usually have a small network diameter [7], [8].

The packet routing delay in utility based forwarding (UTILITY) can be computed using the same logic as in random forwarding (RAND) except that the forwarding probabilities $P_{i,j}^{f}(n)$ in Eqn. 4 need to be reformulated for UTILITY. The forwarding probability in this case can be expressed as:

$$P_{i,j}^{f}(n) = 1, \text{ if } U_{i,d}(n) < U_{j,d}(n), \forall i, j \in N \quad (9)$$

where *N* represents the set of all on-body nodes and where. Eqn. 9 represents a situation in which either node-*i* does not have any neighbor during the n^{th} time slot, or its own utility to the destination node-*d* is higher than those of all its current neighbors. Either way, the node buffers the packet with probability 1. Once the forwarding probabilities are computed applying Eqn. 9 on the on-body topology traces collected in *Section II.C*, the forwarding matrix *A(n)* and the delivery probabilities $\rho_{s,d}^{n}(k)$ are computed using the same rules presented in Eqns. 5 and 6. Finally, the delivery delay is computed as $D_{UTILITY} = \sum_{k=0}^{T} k\left[\prod_{i=0}^{k} A(n+i)\right]_{s,d}$ using Eqn. 7.

D. Probabilistic Routing with Multi-scale Postural Locality (PRMPL)

Routing using PRMPL utilizes a *Postural Link Cost* (PLC) [13] which captures WBAN link localities in multiple time scales. For on-body packet forwarding, the PLC is used exactly the same way as for the UTILITY routing; that is by replacing the utility values by the PLCs. With posture and activity changes of a human subject, the PLC link costs are automatically adjusted such that the packets are forwarded to next-hops which are most likely to provide an end-to-end path with minimum intermediate buffering/storage delays. PLC is defined as $\beta_{i,j}(n)$, $(0 \leq \beta_{i,j}(n) \leq 1)$, which represents the probability of finding $L_{i,j}(n) = 1$. The update equations for PLC are formulated as [13]:

$$\beta_{i,j}(n) = \beta_{i,j}(n) + (1 - \beta_{i,j}(n-1)) \cdot \omega \quad \text{if link } L_{i,j}(n) = 1 \quad (10)$$

$$\beta_{i,j}(n) = \beta_{i,j}(n-1) \cdot \omega \quad \text{if link } L_{i,j}(n) = 0$$

According to Eqn. 10, When the link is connected, the *Postural Link Cost* (PLC) $\beta_{i,j}(n)$ increases at a rate determined by the constant ω $(0 \leq \omega \leq 1)$, and the difference between the current value of $\beta_{i,j}(n)$ and its maximum value, which is 1. As a result, if the link remains connected for a long time, the quantity $\beta_{i,j}(n)$ asymptotically reaches its maximum value of 1. When the link is disconnected, $\beta_{i,j}(n)$ asymptotically reaches zero with a rate determined by the constant ω. To summarize, for a given ω, $\beta_{i,j}(n)$ responds to the instantaneous connectivity condition of the link $L_{i,j}$.

With time invariant ω, the PLC update rules in Eqn. 10 captures the locality in short-term link connectivity in a manner conceptually similar to the age based utility formulation, as developed in [8], [7]. It is, however, not the same because in the designs in [8], [7], the routing utility of a link is increased incrementally when the link is formed, and is reduced to zero as soon as the link is disconnected. This formulation of utility misses out the fact that even after disconnection, the formation probability of that link may be higher than a currently-connected link. In other words, those definitions of utility fairly differentiate across currently connected links, but not across the currently non-connected links. In the formulation of PLC in Eqn. 10, motivated by the logic used in PROPHET [6], we track the short-term locality even when a link is not physically connected. This extended persistency in PLC is expected to improve performance over the existing age based utility definitions as used in [8], [7].

The next design step is to dimension the parameter ω for capturing link localities at a longer time scale. From Eqn. 10, for a high ω (e.g. 0.9), $\beta_{i,j}(n)$ increases fast when the link is connected, and decreases slowly when the link is not connected. Conversely, for a low ω (e.g. 0.1), $\beta_{i,j}(n)$ increases slowly when the link is connected, and decreases fast when the link is not connected. Ideally, it is desirable that for a historically good link (i.e. connected frequently on a longer time-scale), $\beta_{i,j}(n)$ should increase fast and decrease slowly, and for a historically bad link, it should increase slowly and decrease fast. This implies that the parameter ω needs to capture the long-term history of the link; hence it should be link specific and time varying. Based on this observation, we define *Historical Connectivity Quality* (HCQ) of an on-body link $L_{i,j}$ at time slot *n* as: $\omega_{i,j}(n) = \sum_{r=n-T_{window}}^{n} L_{i,j}(r) \Big/ T_{window}$ (11)

The constant T_{window} represents a measurement window (in number of slots) over which the connectivity quality is averaged. The factor $\omega_{i,j}(n)$, $(0 \leq \omega_{i,j}(n) \leq 1)$ indicates the historical link quality as a fraction of time the link was connected during the last T_{window} slots. The parameter T_{window} should be chosen based on the human postural mobility time constants. Experimentally, we found the optimal T_{window} values that work well for a large number of subject individuals and range of postures to be in between 7 sec. and 14 sec.

Fig. 3 shows the evolution of PLC $\beta_{i,j}(n)$ and HCQ $\omega_{i,j}(n)$ with time. The top graph shows an example link activity (indicated by $L_{ij}(n)$) with the first half indicating a steadily connected link with a single time slot (1.4 sec.) of disconnection at time slot 10, and the second half indicates a steadily disconnected link with single slot of connection at the 41^{st} slot. The top graph also shows the evolution of $\omega_{i,j}(n)$ according to Eqn. 11 with a T_{window} set to 7 time slots. The bottom graph shows the evolution of $\beta_{i,j}(n)$ with constant ω (i.e. 0.9 and 0.1) and link-specific time varying

$\omega_{i,j}(n)$ from Eqn. 11, indicating the historical link quality. When the link is steadily well connected (during the first half), a high constant ω (i.e. 0.9) responds well to a momentary disconnection by decreasing $\beta_{i,j}(n)$ slowly, but recovering quickly when the link becomes reconnected. A low constant ω (i.e. 0.1) responds poorly in this situation by doing just the opposite - that is a fast decrease and slow recovery.

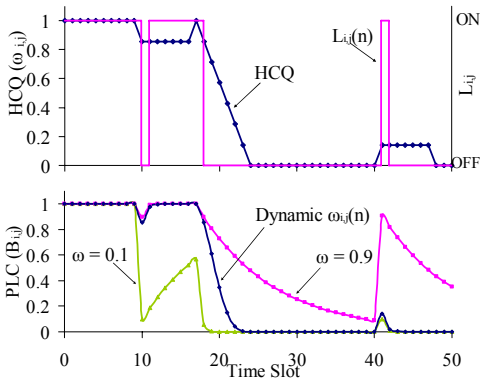

Fig. 3: Evolution of multi-scale locality in terms of PLC and HCQ

Similarly, when the link is steadily disconnected (during the second half), a low constant ω (i.e. 0.1) responds relatively better than a high constant ω (i.e. 0.9) by increasing $\beta_{i,j}(n)$ slowly for a momentary connection, and decreasing $\beta_{i,j}(n)$ quickly after the link becomes disconnected. The lines for two constant ω values clearly show that a single constant value for ω is not able to handle both good-link and bad-link situations equally effectively.

As hypothesized, the link-specific and time-varying $\beta_{i,j}(n)$, on the other hand, is able to handle both situations well by mimicking the behavior of $\omega = 0.9$ during the historically good-link situation, and that of $\omega = 0.1$ during the historically bad-link situation. These results clearly demonstrate the effectiveness of the HCQ and PLC concepts for designing routing utilities that can capture both short and long term localities of the on-body link dynamics. With this multi-scale approach, the proposed mechanism should be able to outperform both age-based (UTILITY) [8], [7] and probabilistic [6] routing protocols that use only short term locality information.

Note that unlike the entities in Fig. 2 , the PLC and HCQ in Fig. 3 show the link connectivity localities which depends on the short and long term history of the link. The localities captures in Eqns. 9 and 11 are responsible for this memory based behavior in Fig. 3 in contrast to the instantaneous link behavior in Fig. 2.

The forwarding rule in PRMPL is identical to what stated for UTILITY based forwarding in *Section C* with the utility function $U_{i,j}(n)$ replaced by the postural link cost $\beta_{i,j}(n)$. Consequently, the forwarding probabilities $P^{f}_{i,j}(n)$, the forwarding matrix *A(n)*, and the delivery probabilities $\rho^{n}_{s,d}(k)$ can be computed using Eqns. 5, 6 and 10 respectively, and finally, the end-to-end packet delay can be computed as $D_{PRMPL} = \sum_{k=0}^{\tau} k \left[\prod_{i=0}^{k} A(n+i) \right]_{s,d}$ using Eqn. 6.

IV. PERFORMANCE EVALUATION

The same seven-sensor laboratory prototype network, as shown in Fig. 1, was used for the on-body experimental evaluation of all the analyzed routing protocols. Results correspond to packets originated from node-3 to the common destination node-6, attached on the right ankle, representing the longest hop (i.e. also worst case) packet routing scenario in most of the body postures. Results are also presented from analytical model, carried out on network topology traces collected during the actual on-body experiments so that the analytical model results can be compared with the experimental data for the exact same topology traces. Those traces are used to create the forwarding matrix in Eqn. 5 for computing the analytical packet delay numbers for all the analyzed routing protocols.

In order to avoid the CSMA MAC collisions inherent to Mic2Dot's TinyOS networking stack, we have implemented a higher layer polling access strategy managed by one on-body node. This polling node polls the other six sensor nodes in a round-robin fashion, so that a regular node forwards packets (both data and Hello) only when it is polled by the polling node and given access to the channel. A polling time frame of 1.4 sec. is used which is divided into 7 time slots, one for each of the seven on-body nodes. Note that the polling node itself also needs to send Hello packets etc. for link cost formulation as described in Section III. Although the data packets and the Hello messages from the nodes are transmitted at software power adjusted transmission range of 0.3m-0.6m, the polling packets are transmitted by the polling node at full power so that all on-body nodes receive such packets.

A. *Performance Metrics and Traffic Generation*

The primary performance index is the end-to-end Packet Delay (PD), which is modeled in this paper and is attempted to be explicitly minimized by the UTILITY and PRMPL protocols as presented in Sections III.C and III.D. One secondary metric, namely, Packet Hop Count (PHC) is also recorded for a more complete understanding. A chosen source node is programmed to generate data packets at the rate of 1 packet every 4 discrete time slots (each slot is 1.4 sec), with a packet size of 46 bytes. All on-body network nodes are slot-level time-synchronized by the sink node (i.e. node-6 in Fig.1) using periodic synchronization packet broadcast at a high transmission power [13].

B. *Packet Delay (PD)*

End-to-end packet delivery delays for a packet from the source node-3 on left upper arm to the sink node-6 on right ankle for all routing protocols analyzed in *Section III* are reported in Fig. 4. For each of these protocols, a separate experiment was run for 1320 sec. (i.e. 22 minutes), sending 230 packets, and spanning 6 different body postures and activities (SIT, SIT-RECLINING, LYING-DOWN, STAND, WALK and RUN), each lasting for 20 sec. Fig. 4 reports the average of packet delay computed from the analytical model and on-body experiment.

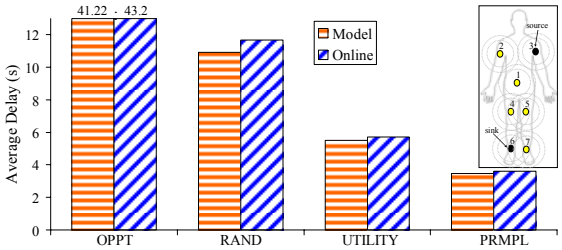

Fig. 4: On-body packet delivery delay for different DTN routing protocols

The following observations can be made from Fig. 4. First, the experimental and model-generated analytical results closely match across all protocols. Second, as a general trend the delay

performance improves with the amount of knowledge leveraged on topological locality. PRMPL achieves significantly better delay compared to the other protocols delay, because it is able to capture multi-scale topological localities in human postural movements using the cost parameters $\beta_{i,j}(n)$, as explained in *Sections III.D.*.

The age based approach UTILITY uses only the short-term locality, which explains its larger delay compared to PRMPL, but smaller delay than OPPT and RAND, both of which do not leverage any topological locality information and responds based solely on instantaneous link conditions. Randomized forwarding provides slightly better delay since in a typically small WBAN, there are only few possible end-to-end path combinations, leading to quicker delivery than the opportunistic mode in which a delivery is possible only when the source directly meets the destination.

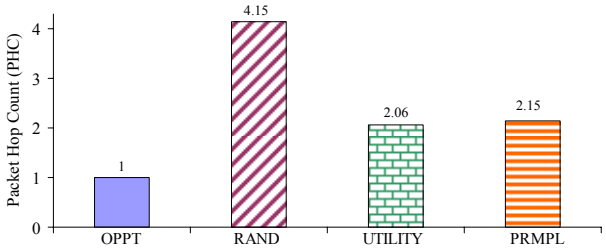

Fig. 5: Average Packet Hop Count

C. *Packet Hop Count (PHC)*

Fig. 5 shows the average PHC which serves as an indirect measure for communication energy expenditure (i.e. for transmission and reception) for the on-body sensors. The large number for RAND explains the impacts of random forwarding compared to all other protocols. Since with the opportunistic routing (OPPT) packets are delivered only when a source comes in direct contact of the destination, all packets are delivered with PHC 1.

D. *Impacts of Postural Stability*

For all the experiments so far, each individual physical posture was made to last for 20 sec. In order to study the impacts of variable postural stability on the routing performance, the subject was instructed to repeat the same sequence of postures as in *Section III*, but with different posture durations ranging from 10 sec. to 40 sec.

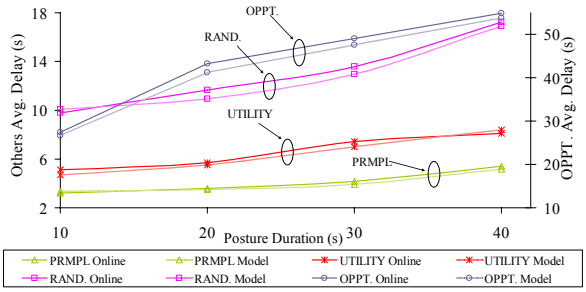

Fig. 6: Impacts of posture duration on packet delay

Fig. 6 shows the impacts of posture duration on average packet delay for all five protocols. Due to its significantly higher values, the packet delays for the OPPT protocol are plotted as a separate axis in Fig. 6. Observe that the packet delays for all the protocols generally increase with higher posture durations. This is because longer posture duration implies that a connected link remains connected for longer duration and also a disconnected link remains disconnected longer. As a result, a packet that is buffered in a node due to network partitioning remains buffered for longer duration, leading to higher end-to-end delay. In a relative sense, all the experimented protocols maintain the same performance trend for packet delay as observed in *Section C*, Fig. 4.

V. CONCLUSION AND ONGOING WORK

This paper develops a delay modeling framework for store-and-forward packet routing in Wireless Body Area Networks (*WBAN*). Using a prototype *WBAN* for experimentally characterizing and capturing on-body topology traces, an analytical delay modeling technique was developed for evaluating single-copy DTN routing protocols. End-to-end routing delay for a series of protocols including opportunistic, randomized, utility based and other mechanism that capture multi-scale topological localities in human postural movements have been evaluated. Performance was evaluated experimentally and using the developed models. It was shown that via multi-scale modeling of the spatio-temporal locality of on-body link disconnection patterns, it is possible to attain better delay performance compared to opportunistic, randomized and utility based DTN routing protocols in the literature. Ongoing work on this topic includes developing a Kalman Filter based body movement prediction model for predictive on-body packet routing with lower delay objectives.

VI. REFERENCES

[1] D. Sagan, "RF Integrated Circuits for Medical Applications: Meeting the Challenge of Ultra Low Power Communication," *Ultra-Low-Power Communications Division, Zarlink Semiconductor*, 2005.

[2] S. Mikami, T. Matsuno, M. Miyama, M. Yoshimoto, and H. Ono, "A Wireless-Interface SoC Powered by Energy Harvesting for Short-range Data Communication," in *Asian Solid-State Circuits Conference, 2005*, pp. 241-244, 2005.

[3] E. Strömmer, M. Hillukkala, and A. Ylisaukkooja, "Ultra-low Power Sensors with Near Field Communication for Mobile Applications," *International Conference on Wireless Network, ICWN'07*, pp. 1-12, 2007.

[4] T. Falck, H. Baldus, J. Espina, and K. Klabunde, "Plug 'n Play Simplicity for Wireless Medical Body Sensors," in *Pervasive Health Conference and Workshops, 2006*, pp. 1-5, 2006.

[5] E. Jones and P. Ward, "Routing strategies for delay-tolerant networks," *ACM Computer Communication (CCR)*, 2006.

[6] A. Lindgren, A. Doria, and O. Schelén, "Probabilistic routing in intermittently connected networks," *SIGMOBILE Mob. Comput. Commun. Rev.*, vol. 7, no. 3, pp. 19-27, 2003.

[7] T. Spyropoulos, K. Psounis, and C. Raghavendra, "Efficient Routing in Intermittently Connected Mobile Networks: The Single-Copy Case," *Networking, IEEE/ACM Transactions on*, vol. 16, no. 1, pp. 63-76, 2008.

[8] H. Dubois-ferriere, M. Grossglauser, and M. Vetterli, "Age matters: Efficient route discovery in mobile ad hoc networks using encounter ages," 2003. [Online]. Available: http://eprints.kfupm.edu.sa/23199/. [Accessed: 02-Dec-2009].

[9] A. Vahdat and D. Becker, "Epidemic Routing for Partially Connected Ad Hoc Networks," *Technical Report CS-200006, Duke University*, 2000.

[10] A. Jindal and K. Psounis, "Performance analysis of epidemic routing under contention," in *Proceedings of the 2006 international conference on Wireless communications and mobile computing*, pp. 539-544, 2006.

[11] T. Spyropoulos, K. Psounis, and C. S. Raghavendra, "Efficient routing in intermittently connected mobile networks: The multiple-copy case," *IEEE/ACM Transactions on Networking (TON)*, vol. 16, no. 1, pp. 77–90, 2008.

[12] J. Leguay, T. Friedman, and V. Conan, "DTN routing in a mobility pattern space," in *Proceedings of the 2005 ACM SIGCOMM workshop on Delay-tolerant networking*, pp. 276-283, 2005.

[13] M. Quwaider and S. Biswas, "Disruption Tolerant Network Routing in Body Sensor Networks with Dynamic Postural Partitioning," *In Press, To Appear, Elsevier Ad Hoc Networks*, 2010.